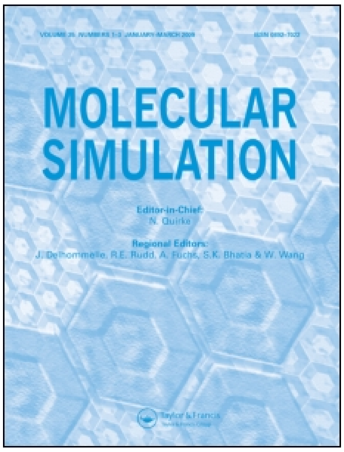

Molecular Simulation
Publication details, including instructions for authors and subscription information:
http://www.informaworld.com/smpp/title~content=t713644482

Finite temperature properties for zinc nanoclusters

K. L. Wu[a]; S. K. Lai[a]; W. D. Lin[a]
[a] Complex Liquids Laboratory, Department of Physics, National Central University, Chung-li, Taiwan

To cite this Article Wu, K. L. , Lai, S. K. and Lin, W. D.(2005) 'Finite temperature properties for zinc nanoclusters', Molecular Simulation, 31: 6, 399 — 403

To link to this Article: DOI: 10.1080/08927020412331332749

URL: http://dx.doi.org/10.1080/08927020412331332749

Molecular Simulation, Vol. 31, Nos. 6–7, 15 May – 30 May 2005, 399–403

Finite temperature properties for zinc nanoclusters

K.L. WU*, S.K. LAI and W.D. LIN

Complex Liquids Laboratory, Department of Physics, National Central University, Chung-li 320, Taiwan

(Received September 2004; in final form October 2004)

The Gupta-type many-body potential was applied to describe the interactions between atoms in zinc nanoclusters. From the calculated ground state structures, obtained by Brownian-type molecular dynamic simulation, we investigated the temperature effect of zinc clusters. We studied in particular the constant volume specific heat C_V which is a thermodynamic quantity and also the relative bond length Lindemann parameter δ which is a geometric quantity. Effort is devoted to revealing the anomalies observed in these quantities for Zn clusters and making a comparison with those of the typical sp-type metallic clusters. To this end, we have chosen to calculate the C_V and δ of clusters Zn_n for $n = 13$, 29, 33, and 53 which are judged to be less stable by the energy difference and the second energy difference as well as 6, 36, 42, and 49 which are judged by the same energy criteria to be relatively more stable. Our results of simulation show that the structures of C_V and δ exhibit unusual phase transition behaviors which are drastically different from those of the usual metallic clusters. General scenarios observed in the simulation are the prevalence of the pre-melting phenomenon predicted in all of the clusters studied here.

Keywords: Thermal property; Nanoclusters; Metallic clusters; Molecular dynamics simulation

1. Introduction

Clusters provide a representative model system to understand finite systems. In recent years, there have been many studies, both theoretical and experimental, that focus on the properties of nanoclusters. The majority of the theoretical studies for metallic clusters aim to calculate the ground state structures. The optimization techniques such as the basin hopping (BH) [1] and the genetic algorithm (GA) [2] are two of the state-of-the-art methodologies widely used to predict the lowest energy values for metallic clusters. Considerable progress has been achieved in understanding the zero temperature structures of clusters. In comparison, lesser works are directed to investigate the thermal properties. It is the purpose of this work to report on the finite temperature effect of the atypical zinc cluster using Brownian-type molecular dynamics (MD) simulation [3].

To account for the many-body interactions between zinc atoms, the Gupta-type empirical potential [4–5] is used. We have previously [6] applied the same potential to alkali metallic clusters and found from the energy difference, ΔE, and the second energy difference, $\Delta_2 E$, (defined below) that these metals show striking regularity in ΔE and $\Delta_2 E$ for all of the alkali metals Na, K, Rb, and Cs and their cluster growth patterns manifest icosahedral or double icosahedral structures. On the other hand, Michaelian *et al.* [7] and Doyle [8] found that zinc cluster displays a very different structure from many typical simple metallic clusters. One noticeable feature is that the Zn cluster fails to follow any high symmetry or ordered global minimum geometry. It is therefore, interesting to investigate the properties of such glassy cluster. Recalling that in the bulk, zinc has an hcp structure with an unusually large *c*/*a* ratio (1.856) and a relatively low melting temperature of 692.5 K. As a result, the phase transition behavior or the melting phenomenon of zinc should be very different from metallic clusters such as the alkali metals whose structures are of high symmetry. By appealing to the Gupta-type many-body potential, we employ the Brownian-type MD simulation [3] to study the thermodynamic and geometric properties of this particular cluster. Our main analysis is to understand the mechanism of the solid–liquid phase transition which is an analogue to the melting behavior in the bulk metal.

This paper is divided into three parts. First, we describe briefly the many-body potential used in this work and document the essential equations used in the Brownian-type MD simulation. Second, we analyze the numerical results and discuss the possible mechanism for the melting

---

*Corresponding author. E-mail: wkol@cliq.phy.ncu.edu.tw

Molecular Simulation
ISSN 0892-7022 print/ISSN 1029-0435 online
http://www.tandf.co.uk/journals
DOI: 10.1080/08927020412331332749

phenomenon. Finally, we give an overall summary of our present study.

2. Theory

2.1 Empirical many-body potential

For a finite system, many-body interactions are important. Here we employ the empirical Gupta-type potential to characterize the many-body effects. This empirical potential which was used in our preceding work [3,6] has five parameters and they were determined by fitting to experimental bulk data. Mathematically, the potential reads

$$E_n = \sum_{i=1}^{n} [V_r(i) - V_a(i)], \tag{1}$$

where n is the number of particles in the cluster. The repulsive term V_r is

$$V_r(i) = \xi \sum_{j \neq i} \exp\left[-p\left(\frac{r_{ij}}{r_0} - 1\right)\right] \tag{2}$$

and the attractive term V_a, due to the hybridization of valence electrons, is

$$V_a(i) = \left(\sum_{j \neq i} \gamma^2(r_{ij})\right)^{1/2}. \tag{3}$$

In equation (2), r_0 is the nearest neighbor distance in the neighborhood of equilibrium bulk inter-atomic distance, and $r_{ij} = |\mathbf{R}_i - \mathbf{R}_j|$ means the separation distance between atoms at positions $\mathbf{R}_i$ and $\mathbf{R}_j$. The $\gamma(r_{ij})$ plays the role of transfer integrals [9,10] and is given by

$$\gamma(r_{ij}) = \varsigma \exp\left[-q\left(\frac{r_{ij}}{r_0} - 1\right)\right] \tag{4}$$

where ς may be defined to be the value of γ at $r = r_0$. The parameters p, q, ξ, ς and r_0 in the potential function are customarily determined by fitting to measured bulk values. For the metal Zn, these parameters are taken from Cleri and Rosato [5] and they are $p = 9.689$, $q = 4.602$, $\xi = 0.1477\,\mathrm{eV}$, and $\varsigma = 0.89\,\mathrm{eV}$.

2.2 Molecular dynamics simulation

To study the thermal properties of a free cluster, we follow our recent work [3] employing a coupling scheme previously proposed by Ju and Bulgac [11]. According to the latter authors, the time evolution of a free cluster embedded in thermal bath at temperature T satisfies the following equations of motion whose x-component reads:

$$\dot{x}_i = \frac{p_{xi}}{m}, \tag{5}$$

$$\dot{p}_{xi} = -\frac{\partial E_n}{\partial x_i} - \frac{\alpha e_0}{nL_0}\mu_x^3 \frac{p_{xi}}{p_0} - \frac{\beta e_0}{nL_0}\nu_x\left(\frac{p_{xi}^2}{p_0^2} - a_0\right) - \frac{\chi e_0}{nL_0}\eta_x \frac{p_{xi}^3}{p_0^3}, \tag{6}$$

$$\dot{\mu}_x = \frac{\alpha T}{p_0 L_0}\left(\frac{\sum_{i=1}^{n} p_{xi}^2}{nmT} - 1\right), \tag{7}$$

$$\dot{\nu}_x = \frac{\beta T}{p_0 L_0}\left(\frac{\sum_{i=1}^{n} p_{xi}^3}{nmTp_0} - a_0 \frac{\sum_{i=1}^{n} p_{xi} p_0}{nmT} - \frac{2\sum_{i=1}^{n} p_{xi}}{np_0}\right), \tag{8}$$

$$\dot{\eta}_x = \frac{\chi T}{p_0 L_0}\left(\frac{\sum_{i=1}^{n} p_{xi}^4}{nmTp_0^2} - \frac{3\sum_{i=1}^{n} p_{xi}^2}{np_0^2}\right), \tag{9}$$

where x_i and p_{xi} are, respectively, the x component coordinate and momentum of the ith particle; the y and z components take on the same form. In equation (6), E_n is the potential energy defined by equation (1), $e_0 \approx mL_0^2\omega_D^2/(4\pi^2)$ is a constant with the dimension of energy, $p_0 = \sqrt{2mT}$ is an average thermal momentum at temperature T in which m is the atomic mass, a_0 is a dimensionless constant, L_0 is a constant with the dimension of length, and μ_x ν_x and η_x are the x-component pseudo-friction coefficients. Note that the magnitude of e_0 is of the order corresponding to free cluster exhibiting a Debye frequency ω_D. The constants $\alpha \approx \beta \approx \chi \approx [mL_0^2/(nTt_0^2)]^{1/2}$ in which $t_0 = 2\pi/\omega_D$ is the smallest characteristic time scale of the system, are cluster independent.

Considering the size of Zn clusters of interest here, we have tested the optimized choice of the parameters: $L_0 = 1\,\text{Å}$, $a_0 = 1$, and $\omega_D = 60 \times 10^{12}\,\mathrm{s}^{-1}$. With this set of parameters, we performed simulation with the time step of $\Delta t = 10^{-14}$ s. Each simulation run at given T was carried out for at least 10^7 time steps. The total simulation time steps is done for at least $t \geq 10^{-7}$ s depending on the size of cluster. For smaller size clusters ($n < 20$) in the low temperature region ($T < 100\,\mathrm{K}$), we found that the time step should be scaled down to $\Delta t = 10^{-15}$ s and runs for 10^8 steps in order to keep the total simulation time steps within the same order. Generally, performing longer time steps in simulation would prevent the cluster yielding unreasonable physical properties and make the choice of parameters in equations (6)–(9).

When the system has reached an equilibrium state, the ensemble average of a physical quantity $A(p', \mathrm{q}')$ may be calculated as

$$\langle A(p', q')\rangle = \lim_{t_{\max}\to\infty} \frac{1}{t_{\max}} \int_0^{t_{\max}} A(p'(t), q'(t))\,\mathrm{d}t \tag{10}$$

where $t_{\max}$ is the period over which the system is in the ergodic state. Having introduced all the essential equations needed in simulation, we proceed to describe the two quantities of interest here. The first quantity is

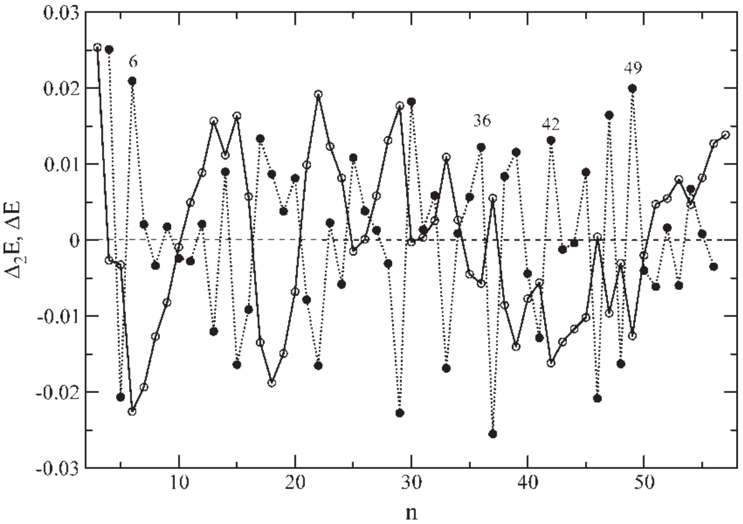

Figure 1. The energy difference ΔE, denoted by open circles, and the second energy difference $\Delta_2 E$, denoted by close circles, plotted against size (n) for zinc clusters. Only magic number clusters are shown.

the constant volume specific heat which is calculated as

$$C_V(T) = \frac{\langle E_{\text{total}}^2 \rangle - \langle E_{\text{total}} \rangle^2}{k_B T^2}, \tag{11}$$

where $E_{\text{total}} = \sum_i p_i^2/(2m) + E_n$ and the $< .. >$ is to be performed using equation (10).

The second quantity is the root-mean-square relative bond length fluctuation δ reflecting the geometric property. δ is defined by

$$\delta = \frac{2}{n(n-1)} \sum\nolimits_{i<j}^{n} \frac{\sqrt{\langle (r_{ij} - \langle r_{ij} \rangle)^2 \rangle}}{\langle r_{ij} \rangle}, \tag{12}$$

which is also known as Lindemann parameter [12]. Physically, when δ changes drastically in some temperature range, it means that the metallic cluster is undergoing some kind of structural phase transition.

3. Results and disscusion

We have applied the Gupta-type potential to calculate the ground state geometry using the numerical technique detailed in our preceding paper [6]. Figure 1 shows the results of the energy difference defined by

$$\Delta E = E_n - (A + Bn^{1/3} + Cn^{2/3} + Dn) \tag{13}$$

The coefficients A, B, C, and D, given by 2.20846, -0.0143308, 0.156717, and $D = -1.36814$, respectively, were determined by least-squares fitting to the lowest energy minima E_n that span over the range $3 \le n \le 57$. Also, we calculate the second energy difference

$$\Delta_2 E = [E_{n+1} - E_n] - [E_n - E_{n-1}] \tag{14}$$

and use it as the stability criterion in our selection of clusters to be studied. In contrast to our previous work [3] we have focused investigation on clusters Zn_n for $n = 13$,

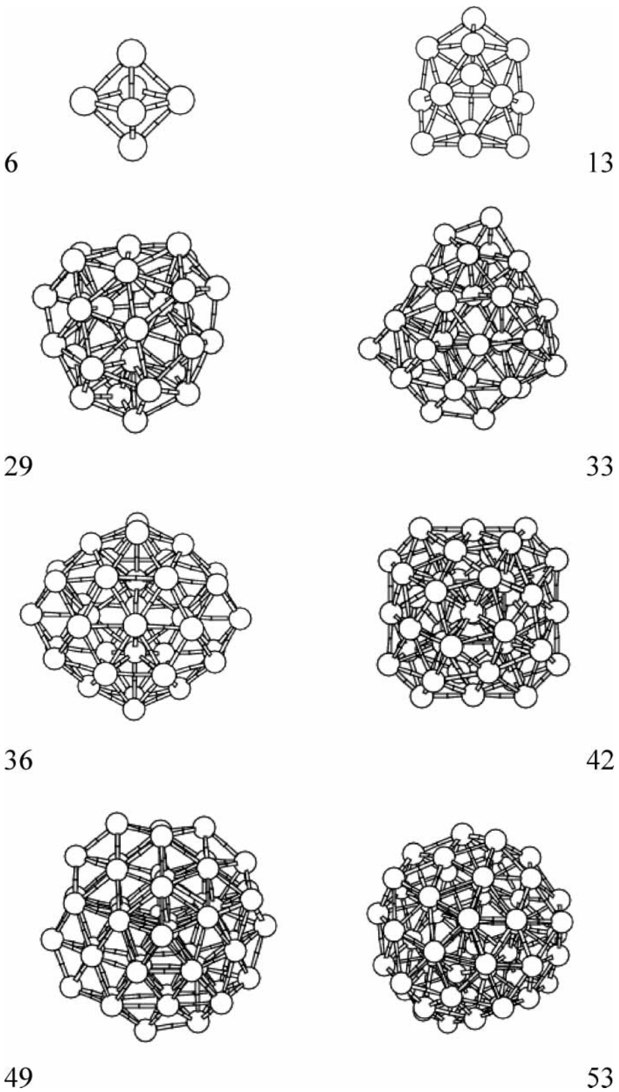

Figure 2. Selected lowest energy structures of zinc clusters.

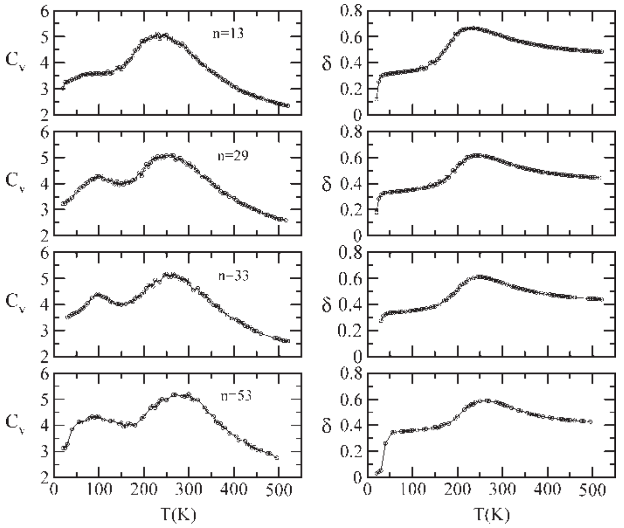

Figure 3. Constant volume heat capacity C_v per atom (in units of k_B) vs. temperature T(K) and root-mean-square relative bond length fluctuation δ vs. temperature T(K) of selected nonmagic number cluster Zn_n for $n = 13, 29, 33$ and 53.

29, 33 and 53. These non-magic number clusters are relatively less stable according to equations (13) and (14). For the purpose of comparison, we have considered also several magic number clusters Zn_n for $n = 6$, 36, 42, and 49. The simulations for all of the clusters begin with their respective ground-state energy configuration shown figure 2 for the magic and non-magic number clusters. The corresponding C_V's are depicted in figure 3 for non-magic clusters and figure 4 for magic clusters along with the δ placed next to them in the same figures. We stress two general scenarios. First, the C_V vs. T curves for all clusters Zn_n, non-magic and magic number (figure 4), show a same pattern—a small pre-peak followed by a broad large principal maximum. Quantitatively, we found that the pre-peak is located at $T \approx 80$ K for Zn_6 and Zn_{13}, but is shifted to higher $T \approx 100$ K for larger size clusters $Zn_{n \geq 29}$. There is observed also in the non-magic number clusters a discernible bump located at $T \approx 50$ K for Zn_{33} and the mild shoulder like bump grows with increasing $n \geq 33$. Similar shifting in the main peak position of $C_V(T)$ is predicted; here for clusters $Zn_{n \leq 29}$, they are located at $T \approx 230$ K and it increases slightly to $T \approx 250$ K for larger clusters $Zn_{n>29}$. The second scenario is the two-steps behavior displayed in all δ vs. T structures. The rise in δ occurs, however, at temperature a little earlier and more rapid for $Zn_{n<33}$. A remarkable characteristic of $\delta(T)$ that we should emphasize is its decreasing behavior beyond the temperature at which the principal peak of $\delta(T)$ is located. This scenario is not observed in other simple metallic clusters previously reported. To understand the first scenario, it is instructive to look first at the cluster Zn_{13}. In most sp-type metallic clusters reported in the literature, this cluster exhibits an icosahedral symmetry and its C_V vs. T shows only unimodal peak which has been unambiguously identified as the solid–liquid-like transition. The appearance of a pre-peak for Zn_{13} thus implies a possibility of geometrical departure from the usual high symmetry ground state structure. This is indeed true as seen in figure 2 where Zn_{13} assumes a disordered structure reminiscing of a geometry of polytetrahedra with surface atoms only. That this is so may be traced to the many-body embedded energy [8] playing a more decisive role compared with the highly symmetric icosahedral ordered structure. Geometrically, the Zn atoms distribute to have lesser coordination number resulting in the reduction of the average atomic density of any zinc atom and hence a lowering of the many-body embedded energy. The additional pre-peak at $T \approx 80$ K simply reflects greater freedom of surface atoms. Physically, it could be due to the presence of isomeric structures [6] where the cluster, under thermal drive, is effecting an oscillatory switch from one well-defined shape to another, or undergoing some form of surface reconstruction or surface melting. It appears that the same distribution pattern of surface atoms applies to Zn_{15} (not shown). As n increases there are slight changes in the arrangement of surface and interior atoms leading to slightly compact (possibly ordered) structure because the pre-peak is observed to displace to $T \approx 100$ K. When the particle size becomes larger still reaching $n = 33$ and 53 (or, for magic number clusters, $n = 36$, 42, and 49) we found the development of a weak shoulder (or apparent and sharper peak for $n = 42$ and $n = 49$) of C_V at a lower $T \approx 50$ K. Nevertheless, all of the Zn_n clusters show either a bimodal or a trimodal structure. Subject to these subtle changes in pre-peaks, the main peak positions at which values the solid–liquid-like transition occurs have accordingly been shifted from $T \approx 230$ K for $Zn_{n \leq 29}$ to $T \gtrsim 250$ K for $Zn_{n>29}$.

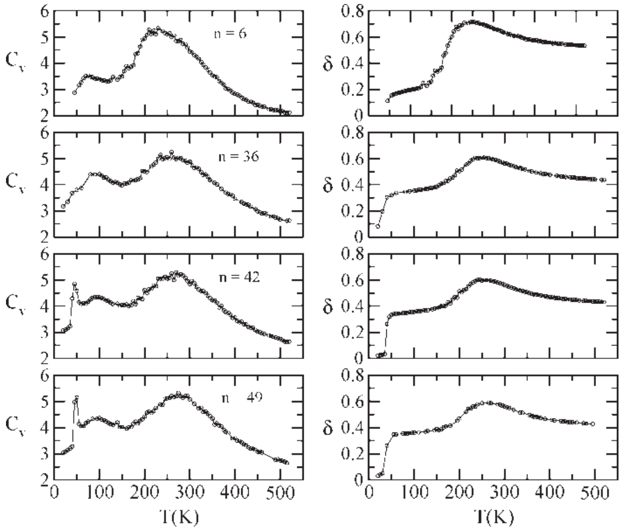

Figure 4. Same legend as figure 3, but selected magic number clusters Zn_n for $n = 6$, 36, 42 and 49.

Coming to the second scenario, we note that the lower temperature at which δ increases rapidly does not quite correspond to the pre-melting temperature in C_V for $Zn_{n \leq 29}$, but for $Zn_{n>29}$, one notices a shoulder like structure which agrees qualitatively (semiquantitatively) with the pre-melting temperature in C_V for nomagic

(magic) number clusters. As a result the increase of $\delta(T)$ in the nonmagic (magic) number clusters is more drastic (milder). Generally, there is, however, a close correspondence between the temperature of the solid–liquid-like transition and the temperature at which δ attains the maximum. The latter temperature may be interpreted to be the occurrence of progressive melting in the sense of increasing diffusivity. There is, however, apparent difference in δ between clusters Zn_n, and say, K_{17} [6]. For although their ground state geometries are disordered, the former shows a clear two-steps structure whereas the latter follows a virtually single-step plateau like structure (see figure 2 in [6]). Since the surface atoms in the outer layer of Zn_n have less coordination number, it is reasonable to anticipate the atoms easily loose-maintaining their thermal vibration as the thermal energy increases. Evidence of this scenario can be gleaned from the detailed studies of Michaelian *et al.* [7] where he found that Zn_n always has several lowest energy isomers. Furthermore, Michaelian *et al.* [7] and Doye [8] also noted that the normally ordered structures are in fact unstable for clusters Zn_n. Finally, we should explain the curious decreasing behavior of $\delta(T)$ for temperature beyond the main maximum. A possible explanation is that more ordered structure is favored at the higher temperature. This conjecture is not unreasonable given that the disordered geometry is generally favorable with respect to ordered structures. Indeed Michaelian *et al.* [7] has compared the ordered and disordered structures of Zn_{38} and deduced from the density functional theory that the disordered structure for Zn_{38} is most stable up to a temperature of slightly over 165 K, after which the f.c.c. truncated octahedral structure is favored. This spectacular result is in qualitative accord with our decreasing $\delta(T)$ for $T > 230$ K.

4. Conclusion

In this work, we reported results of the specific heat and the average bond length fluctuation of metallic clusters zinc obtained using the Brownian-type isothermal MD simulation. We found that zinc clusters considered here show two-stages melting generally. The pre-melting phenomenon is visualized ubiquitously in low temperature region. Possibly, this is due to the low-coordinate surface atoms, which gain thermal energy, deform vibrationally, break away structurally and undergo some kind of surface melting or reconstruction. As the temperature increases further, the solid–liquid-like phase transition occurs with C_V displaying a clear main peak. The temperature range over which the relative bond length fluctuation changes generally does not correspond to temperature at which C_V signals pre-melting. In contrast, δ decreases with increasing temperature beyond its main maximum. This curious scenario is attributed to more ordered structure of the cluster at higher temperature. Further evidences, such as making an inherent structure analysis to reconfirm this δ behavior would be a worthwhile endeavor.

Acknowledgements

We acknowledge financial support from the National Science Council under Contract No. NSC92-2112-M-008-033.

References

[1] D.J. Wales, J.P.K. Doye. Global optimization by Basin-Hoping and lowest energy structures of Lennard-Jones clusters containing up to 110 atoms. *J. Phys. Chem. A*, **101**, 5111–5116 (1997).
[2] N.A. Besley, R.L. Johnson, A.J. Stace, J. Uppenbrink. Theoretical study of the structures and stabilities of iron clusters. *J. Mol. Struct. Theochem.*, **341**, 75–90 (1995).
[3] S.K. Lai, W.D. Lin, K.L. Wu, W.H. Li, K.C. Lee. Specific heat and Lidermann-like parameter of metallic clusters: Mono- and polyvalent metals. *J. Chem. Phys.*, **121**, 1487 (2004).
[4] R.P. Gupta. Lattice relaxation at a metal surface. *Phys. Rev. B*, **23**, 6265–6270 (1981).
[5] F. Cleri, V. Rosato. Tight-binding potential for transition metals and alloys. *Phys. Rev. B*, **48**, 22–33 (1993).
[6] S.K. Lai, P.J. Hsu, K.L. Wu, W.K. Liu, M. Iwamatsu. Structures of metallic cluster: Mono- and polyvalent metals. *J. Chem. Phys.*, **117**, 10715–10725 (2002).
[7] K. Michaelian, M.R. Beltran, I.L. Garzón. Disordered global-minimum structures for Zn and Cd nanoclusters. *Phys. Rev. B*, **65**, 041403 (2002).
[8] J.P.K. Doye. Identifying structural pattern in disordered metal clusters. *Phys. Rev. B*, **68**, 195418 (2003).
[9] F. Ducastelle. Elastic modulus of transition metals. *J. Phys. (Paris)*, **31**, 1055 (1970).
[10] J. Friedel. *Electrons Physics of Metals*, J.M. Ziman (Ed.), Vol. I, Pergamon, London (1969).
[11] N. Ju, A. Bulgac. Finite-temperature properties of sodium clusters. *Phys. Rev. B*, **48**, 2721 (1993).
[12] F.A. Lindemann. The Calculation of Molecular Vibration Frequencies. *Z. Phys.*, **11**, 609–612 (1910).